4

Enhanced Carrier Density in a MoS_2/Si Heterojunction-based Photodetector by Inverse Auger Process

4.1 INTRODUCTION

In recent years, TMDs have established themselves as potential constituents for optoelectronics applications because of their mechanical flexibility and transparency (Baugher et al., 2014; Wang et al., 2012; Zhang et al., 2014). As one of the most influential members of the TMDs family, MoS_2 proves to be of significant importance in the context of optical devices due to its tunable bandgap, high carrier mobility, significant absorption coefficient, the favorable rate of electron-hole (e-h) pair generation, and immense current carrying capacity (Bernardi et al., 2013; Chu et al., 2015; Kim et al., 2012; Liu et al., 2013). In addition, the bandgap tuning in MoS_2 either by changing the number of layers or by electric field facilitates the detection of light at various wavelengths (Lu et al., 2014). A large number of optoelectronic applications based on MoS_2 have already been addressed, for instance, photovoltaic devices, light-emitting diodes, optical modulators, and plasmonic devices (Li et al., 2017; Pospischil and Mueller, 2016; Zhang et al., 2015). Among these applications, the development of hybrid photodetectors based on different vdW heterostructures gains much attention owing to their high performance, including an excellent photo-responsivity and high external quantum efficiency. MoS_2 heterojunction-based photodetectors showed a maximum external photo-responsivity in the range of 8.8×10^2–1.2×10^7 A/W (Lopez-Sanchez et al., 2013; Zhang et al., 2014).

2D layered materials can be used to form a vdW heterojunction with materials of different dimensionalities, such as 0D/2D, 1D/2D, and 3D/2D (Jariwala et al., 2016). The performance of these 2D materials can be significantly enhanced by employing a hybrid heterojunction with other nanomaterials. These hybrid structures prove to be an essential component for commercial applications in optoelectronics and light-harvesting technologies because of their tunable properties and the absence of dangling bonds at the interface (Allain et al., 2015). MoS_2-based hetero-junction has received considerable attention because of its unique electrical and optical properties (Jariwala et al., 2016; Wang et al., 2016). A contact between a few-layer MoS_2 (FL- MoS_2) and n-Si can create a barrier at the interface. The electronic cloud of Mo is to be perturbed by the n-doped silicon Fermi level, resulting in the creation of an energy barrier between them. The formation of an energy barrier between n-Si and n-type ZnO has already been reported in the earlier reports (Ranwa et al., 2014; Ranwa et al., 2014). The photo-induced charge carriers have to overcome this barrier in order to contribute to the photocurrent. As the bandgaps of Si and FL-MoS_2 are 1.1 eV and 1.3 eV, respectively, visible light can excite electrons from both semiconductors. Thus, the photo-induced electrons from MoS_2 and Si can contribute to the total photocurrent. However, as the wavelength varies from visible to infrared region, the photocurrent is reduced due to the insufficient photo energy to cross the barrier. Moreover, despite their great potential, FL-MoS_2 has not been extensively studied, and most of the research is focused only on monolayer MoS_2. In this study, we choose FL-MoS_2 because of its higher absorption rate of incident photons, large current carrying capacity, a higher density of states, and favorable mobility.

The principle of photodetectors is based on the generation and recombination of e-h pairs at the junction. Hence, it is essential to understand the charge transport mechanism in photodetectors in order to investigate the optical behavior of the device. Although there are

several reports on the relaxation process of photo-induced charge carriers in 2D materials, the principal scattering mechanism still remains elusive. The photo-induced charge carriers at the MoS_2/Si heterojunction release their energy either by carrier-carrier interaction or by phonon emission (Lee et al., 2016). In carrier-phonon scattering, the photo-induced charge carriers release their energy in the form of heat while, secondary electrons are generated by photo-induced charge carriers in carrier-carrier interaction. Tielrooij et al. (Tielrooij et al., 2013) pointed out that carrier-carrier interaction is the dominant mechanism in 2D materials through which the photo-induced carriers release their energy.

When exploring the charge transport in the MoS_2/Si heterojunction, it is imperative to understand the contribution of different carrier interactions and scattering mechanisms in the conduction process. Here, we demonstrate a photodetector based on MoS_2/Si vdW heterojunction. The vdW heterojunction was achieved by mechanically exfoliating the FL-MoS_2 and stacking it over the Si substrate (Huang et al., 2015). Earlier reports (Li et al., 2014; Zhong et al., 2015) have also investigated the MoS_2/Si based heterojunction, but these reports lack to give a deep insight into the charge transport mechanism. Also, the tuning of barrier height at the MoS_2/n-Si interface has not been studied thoroughly. Therefore, in this chapter, we present the tuning of barrier height at the MoS_2/n-Si interface with photoexcitation of different wavelengths, which was interpreted by using Bardeen's model. The increase in carrier density due to photon energy results in a reduction of barrier height at the heterojunction. Because of increase in carrier density with wavelength, it was observed that inverse Auger process prevails for relaxation of photo-induced charge carriers at the MoS_2/Si interface over other scattering mechanisms. We present a comprehensive study of charge transport, particularly focusing on Auger-type relaxation processes. The Auger recombination processes are a three-particle mechanism in which the coulomb-mediated transition results in a considerable increase in carrier density (Califano, 2009). These excess photo-induced charge carriers contribute to the increment of the photocurrent (Zhong et al., 2015). The obtained results indicate an efficient photoexcitation at MoS_2/Si heterojunction that may pave the way for new generation photodetectors.

4.2 FABRICATION AND CHARACTERIZATION OF MoS_2/Si HETEROJUNCTION

4.2.1 Fabrication of MoS_2/Si heterojunction

We deposited a Si_3N_4 thin layer of 300 nm on the p- and n-type Si substrate having resistivity 1-10 Ω, using the RF magnetron sputtering technique. A Si_3N_4 target (99.9 % purity) was used for thin film deposition in the presence of 45 sccm of Ar and 10 sccm of N_2 at room temperature. RF power applied to the target was 90 W with a chamber pressure of 2.2×10^{-2} mbar. A 200/5 nm thick Au/Cr for making top contact and a 200 nm thick Al for making bottom contact were deposited on the Si_3N_4/Si structure by thermal evaporation. Au and Al make an ohmic contact with FL-MoS_2 and n-Si, respectively. While p-Si makes an ohmic contact with Al after annealing the sample for 15 min at ~ 300˚C in N_2 ambiance. A geometric pattern is formed on the Au/Cr/Si_3N_4/Si structure by using UV lithography (Suss MicroTec MJB4) with the help of an optical mask, as shown in Figure 4.1(a).

The MoS_2/Si heterojunction is formed by mechanically exfoliating MoS_2 from a commercially available crystal of molybdenite (SPI Supplies) using the scotch tape as the transfer medium. The MoS_2 loaded scotch tape is brought in contact with silicon substrate in order to transfer some of the exfoliated MoS_2 flakes on the silicon. To maximize the contact area between MoS_2 and silicon, the substrate was annealed for 2 min at 100˚ C without peeling off the tape. Finally, the stacked heterojunction between MoS_2 and silicon was achieved by removing the scotch tape from the silicon substrate.

4.2.2 Characterization of MoS_2/Si heterojunction

The thickness of deposited FL-MoS_2 was confirmed with Renishaw Raman spectroscopy with a laser excitation wavelength of 514 nm. Park atomic force microscopy (AFM) imaging system was also used to validate the results obtained by Raman spectroscopy. Figure 4.1(b) shows the Raman spectrum of the exfoliated MoS_2 flake, representing two prominent vibrational modes E^1_{2g} (in-plane) and A_{1g} (out-of-plane) at approximately 384 and 408 cm^{-1}. The difference between the two peaks (~ 24 cm^{-1}) confirms a few-layer nature of MoS_2 (Lee et al., 2012). The absolute thickness (~ 4 nm) of the exfoliated FL-MoS_2 layer on top of p-Si substrate is also confirmed by atomic force microscopy (AFM) and the height profile taken along the dotted line in the AFM image is shown in Figure 4.2(a and b). Another sample having a similar thickness over n-Si was chosen for comparative study. The AFM image and the height profile of the MoS_2/n-Si are shown in Figure 4.3(a and b). The thickness of mechanically exfoliated MoS_2 varies from sample to sample. Therefore, we have made many devices of n- and p-Si each. And we have deliberately chosen those devices for which the thickness of MoS_2 is the same, so that a comparative study is possible. The same kind of results is also obtained on another set of devices.

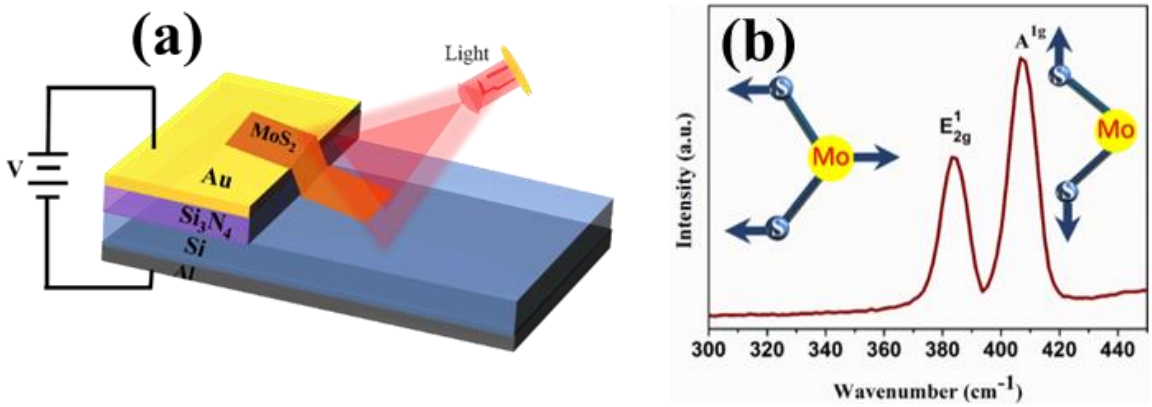

Figure 4.1: (a) Three-dimensional model of FL-MoS_2 photodetector with an experimental setup, (b) Raman spectrum of mechanically exfoliated FL-MoS_2 flake, (c) AFM image of FL-MoS_2 flake on a Si surface forming a heterojunction, and (d) the height profile taken along the dotted line in the AFM image.

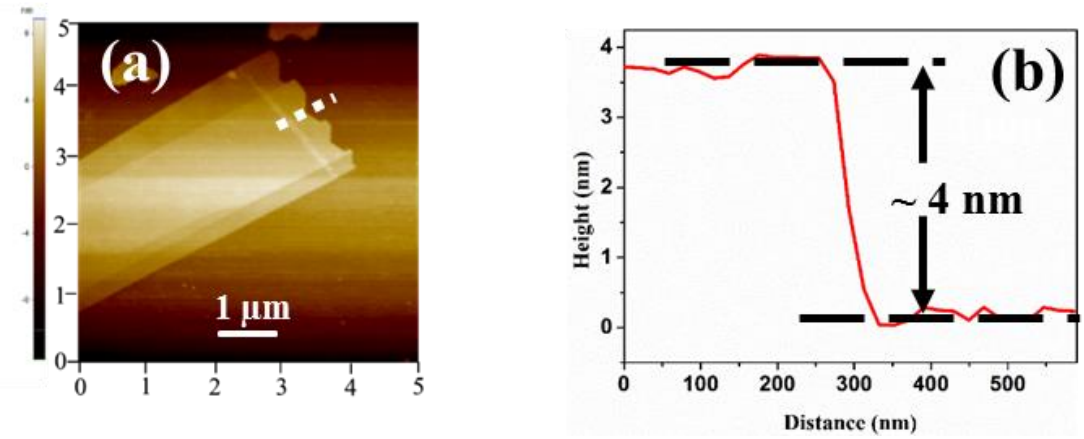

Figure 4.2: (a) AFM image of FL-MoS_2 flake on a Si surface forming a heterojunction, and (b) the height profile taken along the dotted line in the AFM image.

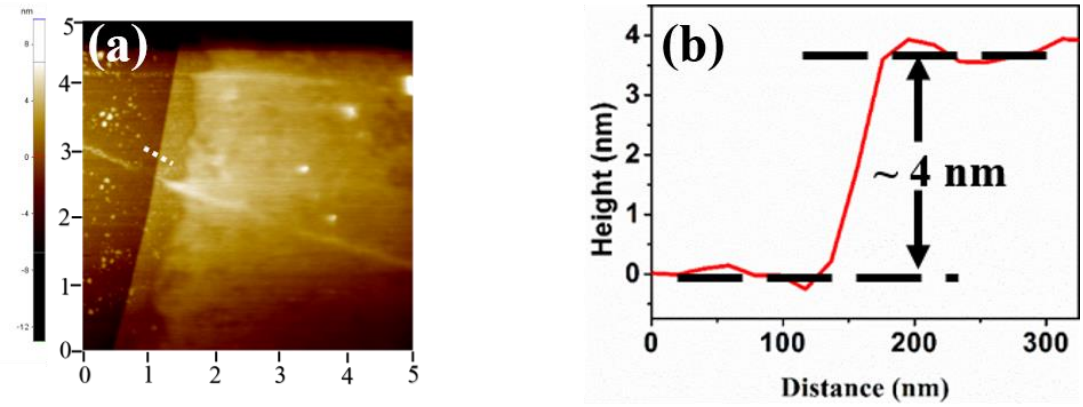

Figure 4.3: (a) AFM image of FL-MoS_2 flake on a Si surface forming a heterojunction, and (b) the height profile taken along the dotted line in the AFM image.

4.3 PERFORMANCE OF THE FABRICATED PHOTODETECTOR

To evaluate the photovoltaic performance, the MoS_2/Si heterojunction was exposed to blue (460 nm), green (520 nm), and red (620 nm) LEDs with an irradiation intensity of 74 mW/cm^2. The electrical measurement was performed using a Keithley 4200 semiconductor characterization system at room temperature. The current-voltage characteristic of the MoS_2/Si heterojunction for both p-Si and n-Si devices in the dark and under light irradiation at wavelengths of 460, 520, and 620 nm with an irradiation intensity of 74 mW/cm^2 is shown in Figure 4.4(a and b). The dark currents of ~ 4.8 µA and ~ 0.45 µA were measured at -4 V for p-type and n-type devices, respectively, which increase with increasing the wavelength of the incident light. The performance of photodetector is measured by its spectral responsivity and detectivity. The spectral responsivity, which is an evaluation of the spectral response of the photodetector, was calculated according to the following equation (Chou et al., 2014):

$$R(\lambda) = \frac{I_L - I_d}{AP_i} \qquad (4.1)$$

where I_L and I_d are currents under light irradiation and in the dark, respectively, A is the active area (12 µm^2) of the heterojunction, and P_i is the incident optical power intensity (74 mW/cm^2). The fabricated MoS_2/Si photodetector exhibits high photo-responsivities of greater than 10^3 A/W for both p-type and n-type devices at -4V. On the other hand, detectivity, which represents the photodetector sensitivity, is calculated by the following expression (Choi et al., 2012):

$$D^* = \frac{A^{1/2}R(\lambda)}{(2qI_d)^{1/2}} \qquad (4.2)$$

By using Eq. (4.2) a detectivity of the order of 10^{12} Jones was achieved for both n-Si and p-Si devices, which is two orders of magnitude higher than other MoS_2 based photodetectors, as shown in Table 4.1. The high detectivity confirms that our MoS_2/Si based photodetector is very sensitive even for a very small optical signal. Table 4.2 lists the photocurrent ($I_{ph}=I_{excited}-I_{dark}$), spectral responsivity and detectivity at MoS_2/Si (n-n and n-p) heterojunctions under the dark condition and with a wavelength of 460, 520, and 620 nm light irradiation. This high photo-responsivity of the fabricated photodetector is attributed to an increased absorption rate of incident photons by FL-MoS_2. While the low value of dark current and high value of photo-responsivity ascribed to the large value of detectivity. The high value of dark current in p-Si device results in a low value of detectivity as compared to the n-Si device. To rule out the possibility of wavelength-dependent photoresponse in Si, the I-V characteristics of pure Si without MoS_2 (only Si and Al contacts) are shown in linear scale (Figure 4.5) and log scale (Figure 4.6), which demonstrate an ohmic behavior. It was observed that visible light irradiation

of different wavelengths does not show any significant impact on the *I-V* characteristics of pure silicon.

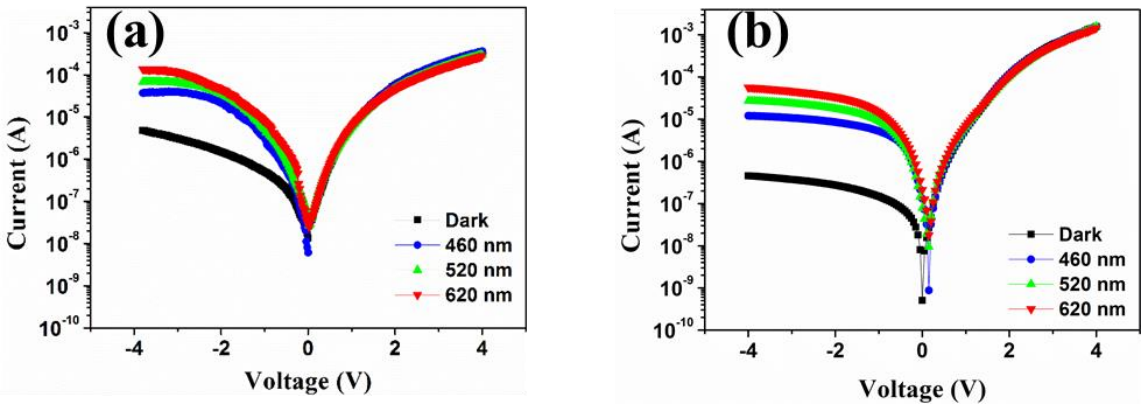

Figure 4.4: I-V characteristics of the MoS_2/Si heterojunction in the dark and under light irradiation of different wavelengths for (a) p-type and (b) n-type devices.

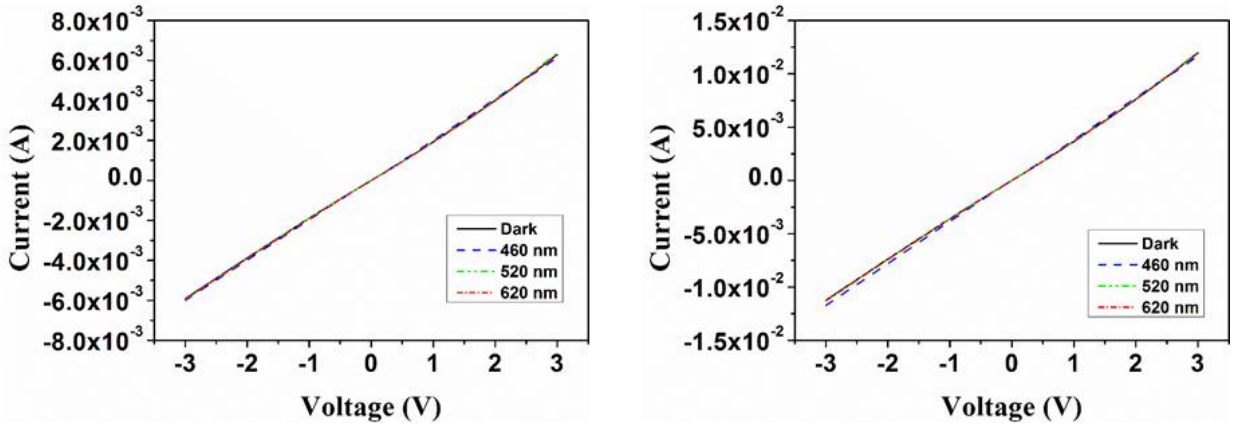

Figure 4.5: The I-V characteristics of pure Si only with Al contacts in the dark and under light irradiation of different wavelengths using a linear scale for (a) p-Si (b) n-Si device.

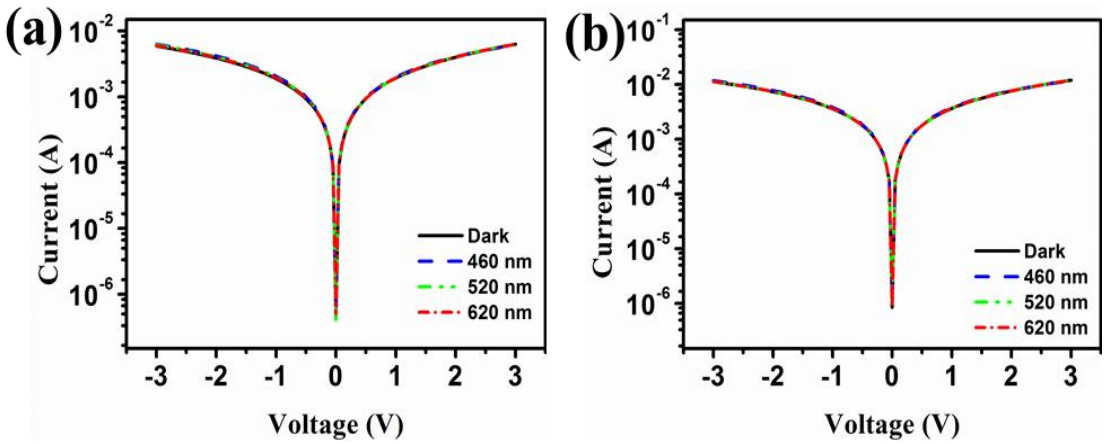

Figure 4.6: I-V characteristics of pure Si only with Al contacts in the dark and under light irradiation of different wavelengths using a log scale for (a) p-Si (b) n-Si device.

Table 4.1: Performance comparison of our MoS_2/Si heterojunction-based photodetector with the MoS_2 -based photodetectors in literature

Device	Spectral range	Responsivity [AW^{-1}]	Detectivity [Jones]	Ref.
MoS_2/Si heterojunction	Visible	~10^3	~10^{12}	This work
MoS_2 as Schottky metal–semiconductor–metal (MSM) photodetectors	Visible	0.57	10^{10}	(Tsai et al., 2013)
Local-gate multilayer MoS_2 phototransistors	Visible	342.6	–	(Kwon et al., 2015)
monolayer MoS_2 phototransistors	Visible	880	–	(Lopez-Sanchez et al., 2013)
MoS_2 p–n diode	Visible-Infrared	5.07	5×10^{10}	(Choi et al., 2014)
Si/monolayer-MoS_2 Heterostructures	Visible	7.2	10^9	(Li et al., 2014)
Aminopropyltriethoxysilane (APTES)/MoS_2 transistors	Visible	5.75×10^3	4.47×10^9	(Kang et al., 2015)

4.4 AUGER AND INVERSE AUGER RELAXATION PROCESSES

In this study, the generation of secondary electrons by a carrier-carrier interaction takes place via two processes. The first one is Auger process, under the 460-nm photo-excitation, an electron transferred its energy to another electron through scattering, while making a transition from the conduction band to the valence band (Califano, 2009; Winzer et al., 2010). The transfer of energy excites an electron from energetically lower state to energetically higher state within the conduction band, as shown in Figure 4.7(a). However, as the wavelength increases from 460 to 620 nm, the decay of hot electrons through inverse Auger process starts dominating over Auger process. Here, the electron makes a transition from an energetically higher state to energetically lower state within the conduction band, while exciting the electron from the valence band into the conduction band, generating an extra e-h pair (Figure 4.7(b)) (Califano, 2009; Winzer et al., 2010).

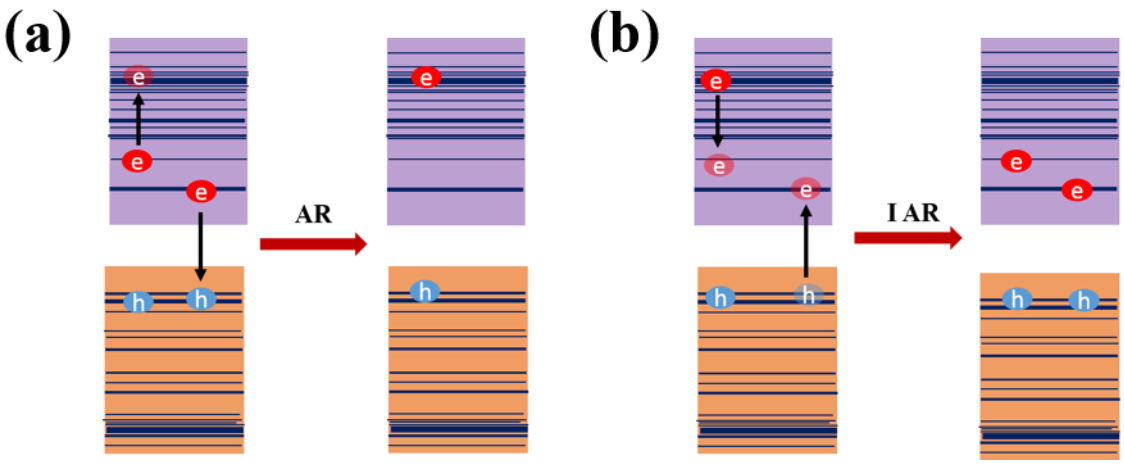

Figure 4.7: Schematic illustration of two Auger-type relaxation processes: (a) Auger recombination (AR) and (b) inverse Auger recombination (IAR) resulted from photon absorption on MoS_2/Si heterojunction.

As a consequence of these secondary charge carriers generated by inverse Auger process, the carrier density increases across the heterojunction. At MoS_2/n-Si heterojunction, the increased carrier density leads to the uprising of the quasi-Fermi level of carriers, resulting in lowering the barrier height and increasing the photocurrent (Azulai et al., 2012). Enhanced photocurrent could be due to inverse Auger recombination or impact ionization. Therefore, it is of crucial importance to check whether impact ionization is efficient enough to give increase the carrier concentration despite the competing processes of inverse Auger recombination. Based on microscopic calculations within the density matrix formalism, Winzer et al. have proved that inverse Auger process generates e-h pairs leading to an increase of the charge carrier density, which results in increasing the photocurrent(Winzer et al., 2010). And it has been found out that this process makes an exceptionally strong contribution to the relaxation dynamics of photo-induced charge carriers in graphene. To prove that their interpretation is correct, they switched off all Auger contributions and obtained constant carrier densities after photoexicitation. The constant current density signifies that the inverse Auger process play a dominant role in increasing the carrier density. Califano et al. (Califano et al., 2004) have also demonstrated that two e-h pairs are likely to be generated from a single photo-induced charge carrier due to inverse Auger process in CdSe nanocrystals. In our work also, the inverse Auger process increases the carrier density by creating more number of e-h pairs at the heterojunction, which agrees very well with the higher value of photocurrent with increase in wavelength.

4.5 CALCULATION OF BARRIER HEIGHT AT THE HETEROINTERFACE

At the MoS_2/n-Si interface, the increase in carrier density with an increase in wavelength from 460 to 620 nm is validated by calculating the barrier height. The tuning of the barrier height at the MoS_2/n-Si heterojunction by light irradiation of different wavelengths is explained by Bardeen's model (Ranwa et al., 2014; Zhang and Harrell, 2003). In this model, the barrier height decreases linearly as the electric field at the junction is increased, and the reverse current can be modeled as:

$$I_0 = I_s\, e\left(\frac{\beta\sqrt{V_r}}{kT}\right) \tag{4.3}$$

where β is the interface parameter and I_s is reverse saturation current that can be calculated as

$$I_s = A\,A^*T^2\,e\left(-\frac{q\Phi r}{kT}\right) \tag{4.4}$$

where V_r, k, T, A, A^*, and Φ_r are the magnitude of applied reverse voltage, Boltzmann constant, operating temperature (300 K), the active area of the fabricated device, effective Richardson constant (112 A/cm^2.K^2 for n-Si), and reverse barrier height, respectively. By using the exponential curve fitting to the experimental data (Figure 4.8(a)), reverse barrier height for the n-Si device was calculated under light irradiation of different wavelengths (Table 4.2). The barrier height of the n-type device is 0.473 eV in the dark state, which decreases to a value of 0.402 under the light irradiation of a wavelength of 620 nm. From Figure 4.4(b), it was observed that at the MoS_2/n-Si interface the current density increases to a value of 4.73×10^6 A/m^2 at 620 nm light irradiation from a value of 3.75×10^4 A/m^2 under dark state at -4V, which is consistent with the lower barrier height observed under 620 nm light irradiation. Newton et al. (Newton et al., 2006) have also found that light irradiation converts ZnO tetrapod Schottky photodiode to ohmic behavior from a rectifying behavior. A quantitative study has also been done by Lu *et al.*(Lu et al., 2015) for illumination induced reduction in barrier height due to increase in carrier density.

Figure 4.8(b) shows the calculated values of spectral responsivity and detectivity under light irradiation of different wavelengths. It was observed that responsivity and detectivity increase for both p-Si and n-Si devices as the wavelength increases from 460 to 620 nm. Moreover, a higher value of photocurrent at 620 nm photo-excitation compared to 460 and 520 nm photo-excitation in both p- and n-type devices, reveal the presence of higher carrier density.

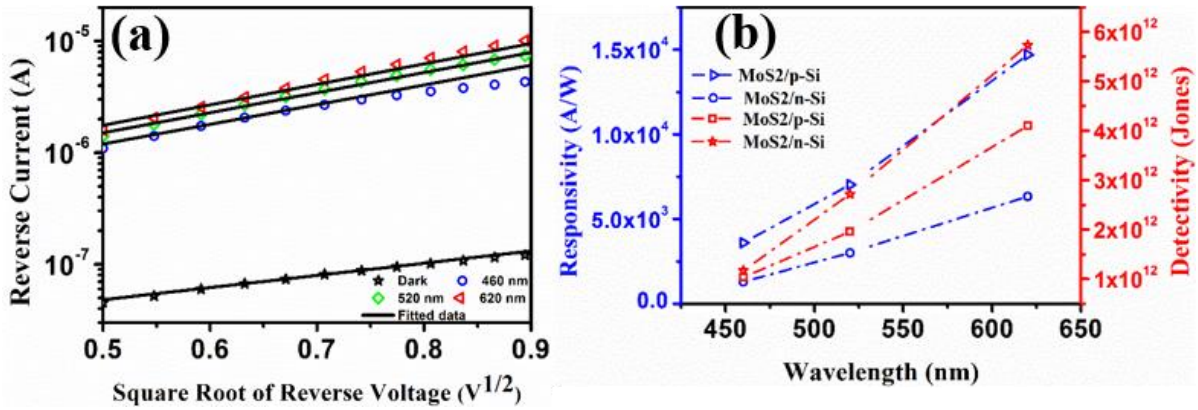

Figure 4.8: (a) Fitting of experimental data of the n-Si device to Eq. (4.3) in the dark and under light irradiation of different wavelengths. The symbols are experimental data points, and solid lines are fitted to the data according to Bardeen's model. (b) Calculated responsivity and detectivity at different wavelengths.

Table 4.2: Photocurrent, Detectivity, Barrier height, and Spectral responsivity of the MoS_2/Si heterojunction at different wavelengths

Wavelength (nm)	Substrate	Photo-current (A)	Detectivity (Jones)	Barrier height Φ_{Bn} (eV)	Spectral responsivity (A/W)
In the dark	p-Si	–	—	—	–
460	p-Si	3.20×10^{-5}	1.04×10^{12}	—	3.6×10^3
520	p-Si	6.24×10^{-5}	1.96×10^{12}	—	7.03×10^3

620	p-Si	1.30×10^{-4}	4.10×10^{12}	–	1.47×10^{4}
In the dark	n-Si	–	–	0.473	–
460	n-Si	1.15×10^{-5}	1.17×10^{12}	0.410	1.30×10^{3}
520	n-Si	2.67×10^{-5}	2.72×10^{12}	0.405	3.01×10^{3}
620	n-Si	5.63×10^{-5}	5.73×10^{12}	0.402	6.34×10^{3}

The photo-induced electrons are generated by the transition from the valence band to the conduction band due to the absorption of high energy photons at the interface. The high energy electrons release their energy in multiple charge carrier generation at the MoS_2/Si interface because of impact ionization and Auger scattering processes (Lee et al., 2016). The effect of carrier multiplication is more pronounced in FL-MoS_2 as compared to monolayer MoS_2 owing to its higher density of states. Califano (Califano, 2009) proposed a direct carrier multiplication model for very high energy photons, and the absorption of a photon with $h\omega > 2E_g$ generates highly excited e-h pairs according to this model. If the excess energy of these electrons exceeds the bandgap energy, then it can be transferred by the coulomb-mediated transition to a valence electron and generates an additional e-h pair.

4.6 TRANSIENT RESPONSE AT MoS_2/Si HETEROINTERFACE

The transient response measurement of the device under different wavelengths light irradiation was done at a fixed voltage bias of -2 V, as shown in Figure 4.9(a and b). The light source was turned on/off regularly to measure the time-dependent response of the photodetector. A nearly identical rise time/decay time was observed for multiple cycles at different wavelengths. The rise time/ decay time estimated to be 135/142 ms for the p-Si device, whereas for the n-Si device the measured value of rise time/ decay time was 132/137 ms, respectively.

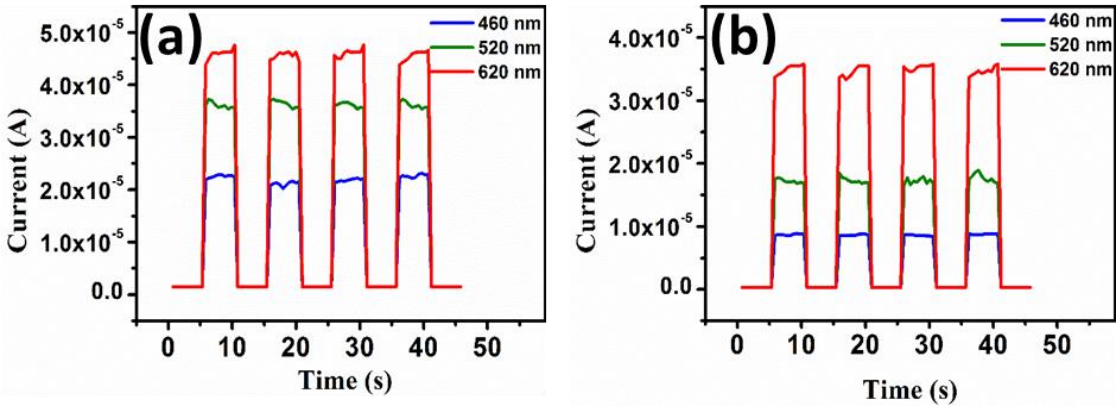

Figure 4.9: Photoswitching characteristic under different wavelength light irradiation at the bias voltage of -2 V (a) p-Si (b) n-Si device.

4.7 CARRIER TRANSPORT ACROSS THE MoS_2/Si HETEROINTERFACE

The movement of charge carriers at the MoS_2/Si interface can also be explained by the energy band diagram. The conduction and valence bands of p- and n-type Si and FL-MoS_2 are properly aligned. When a heterojunction is formed between p-Si and n-MoS_2, a large potential barrier is developed at the interface, which gets further enhanced under the reverse bias, as shown in Figure 4.10(a). The Fermi level of p-Si moves upwards by applying a reverse bias at the heterojunction (Figure 4.10(a)). This upward movement in the Fermi level increases the electric field across the depletion region which expands the barrier potential at the heterojunction. This large potential barrier across the heterointerface assists in separating the e-

h pairs generated due to light irradiation. The energy band diagrams of MoS_2/p-Si and MoS_2/n-Si heterojunctions under reverse bias condition are shown in Figures 4.10(a and b).

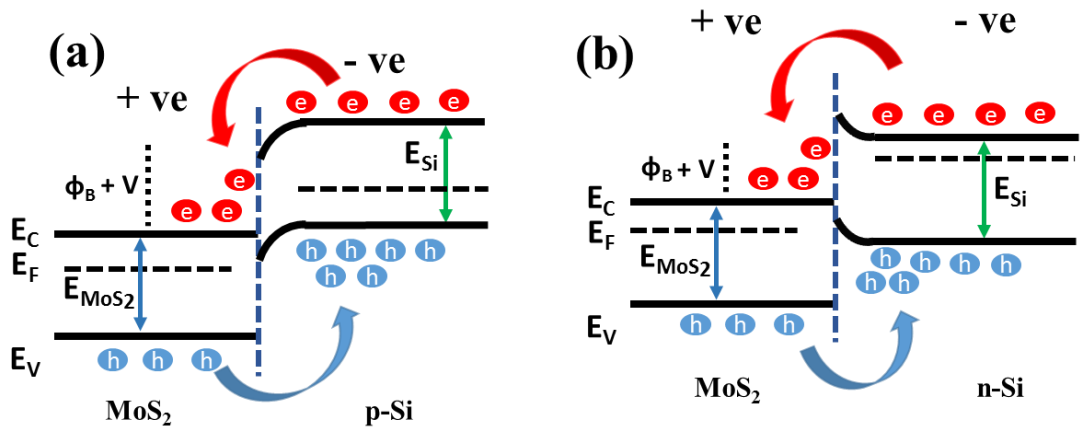

Figure 4.10: Energy band diagram of (a) MoS_2/p-Si and (b) MoS_2/n-Si at heterojunction interface under reverse bias condition under photo-excitation. The arrows indicate the transport of electrons and holes across the heterojunction.

Under visible light irradiation, as the wavelength increases from 460 to 620 nm, multiple charge carriers are generated by absorption of a single photon due to the inverse Auger process, which leads to a considerable increase of the carrier density at the interface. As the electric field of the depletion region increases, it results in the increase of the drift velocity of free charge carriers. This increased velocity helps minority carriers to cross the junction and to increase the photocurrent. This achieved photocurrent is the result of very high drift velocity and a very low recombination rate of photo-induced charge carriers in the depletion region. The photo-induced charge carriers generated outside the depletion region do not play a significant role in photocurrent generation due to a high chance of their recombination and a very low drift velocity.

4.8 CHAPTER SUMMARY

In summary, the MoS_2/p-Si (n-p) and MoS_2/n-Si (n-n) heterojunctions-based photodetectors were fabricated, and the charge carrier relaxation processes at the interface were investigated. The impact of the inverse Auger process on the carrier dynamics of MoS_2/Si heterojunction has been addressed thoroughly. Similar rectifying behavior for both n-type and p-type devices was observed in this study. It was found that the inverse Auger process starts dominating at longer wavelengths, which results in the increase of the carrier density at the interface. The increase in carrier density was validated by calculating the barrier height at the MoS_2/n-Si heterojunction using Bardeen's model. A lower barrier height at higher wavelengths exposes the signature of increase in carrier density due to inverse Auger process at the heterojunction.

we have demonstrated an ultrasensitive photodetector based on MoS_2/Si (for both p- and n-type Si) heterojunction which provides a high photo-responsivity of greater than 10^3 A/W along with a large detectivity of $\approx 10^{12}$ Jones. This high photo-responsivity is attributed to the high absorption rate of incident photons and large current carrying capacity of few-layer MoS_2. A large photo-responsivity with a higher detectivity depicts that the fabricated devices can sense even a small optical signal, making them a potential candidate for the future generation of optoelectronic devices.

…